Cloud Publications
International Journal of Advanced Remote Sensing and GIS
2014, Volume 3, Issue 1, pp. 532-543, Article ID Tech-248
ISSN 2320 - 0243

Research Article | Open Access

Estimation of Evapotranspiration using MODIS Sensor Data in Udupi District of Karnataka, India

G. Dinesh Kumar, B.M. Purushothaman, M.S. Vinaya, and S. Suresh Babu

Department of Civil Engineering, Adhiyamaan College of Engineering, Hosur, Tamil Nadu, India

Correspondence should be addressed to G. Dinesh Kumar, dineshkumaran10@gmail.com

Publication Date: 30 April 2014

Article Link: http://technical.cloud-journals.com/index.php/IJARSG/article/view/Tech-248

Abstract The paper focuses on the estimation of evapotranspiration in the Udupi district, Karnataka using MODIS sensor images. Surface Energy Based Algorithm for Land was utilized for the purpose. Satellite measurements were compared with the concurrent measurements made from meteorological data. Good fit (r^2 = 0.96) between 2 data sets with significant positive correlation (r = 0.97) is observed. The evapotranspiration values range between 85 mm and 1230 mm in the study area. Lower values are reported in December & higher values in June with vegetated plains in the foot belt of Western Ghats showing maximum evapotranspiration.
Keywords *Evapotranspiration; NDVI; Remote Sensing; SEBAL*

1. Introduction

Evapotranspiration (ET) is a combined process of evaporation of liquid water from various surfaces, transpiration from the leaves of plants and trees, and sublimation from ice and snow surfaces. It is a major part of water cycle and is an important factor in understanding the complex feedback mechanisms between the earth's surface and the surrounding atmosphere. Approximately 62% of the precipitation over continents is evapotranspired on an annual scale (Shiklomanov and Sokolov, 1983; Dingman, 1994).

A number of models for ET estimation have been developed which include empirical, semi-empirical and physical models. These models have increased the precision of ET estimation (Brutsert, 1979). There are many methods available to estimate reference ET using meteorological data such as FAO-24 (Doorenbos and Pruitt, 1977), FAO-56 (Allen et al., 1998). Reference ET can be defined as the ET rate of a reference crop expressed in inches or millimeters. Most of these methods are based on point data, which do not provide a good estimation of ET for large areas. The problem of actual ET estimation over a large area can be solved using remote sensing methods that provide ET on pixel by pixel basis. Many researchers (Vidal and Perrier, 1989; Bastiaanssen, 1995; Granger, 1997; Allen et

al., 2007) have worked on developing models by integrating satellite images and weather data on regional scale.

Factors that affect evapotranspiration include the plant's growth stage or level of maturity, percentage of soil cover, solar radiation, humidity, temperature and wind. Isotope measurements indicate transpiration is the larger component of evapotranspiration (Williams et al., 2004).Sensible heat flux is estimated from wind speed and surface temperature using a unique internal calibration of the near surface-to-air temperature difference as described by (Bastiaanssen et al., 1998a). The objective of the present study is to estimate the evapotranspiration in the Udupi district of Karnataka by integrating Remote Sensing and SEBAL Algorithm.

2. Study Area

Udupi district is bound by Arabian Sea in west and Western Ghats in the east. Land bordering Western Ghats in the east is covered with forests and hilly terrain. The district is harboring rare species of flora and fauna. The area geographically lies between 13˚26´N & 13˚80´ N latitudes and 74˚63´ E & 75˚41´ E longitudes. The area enjoys a heavy rainfall of 3000–4000 mm per annum. The temperature varies from 18–38^{o}C.

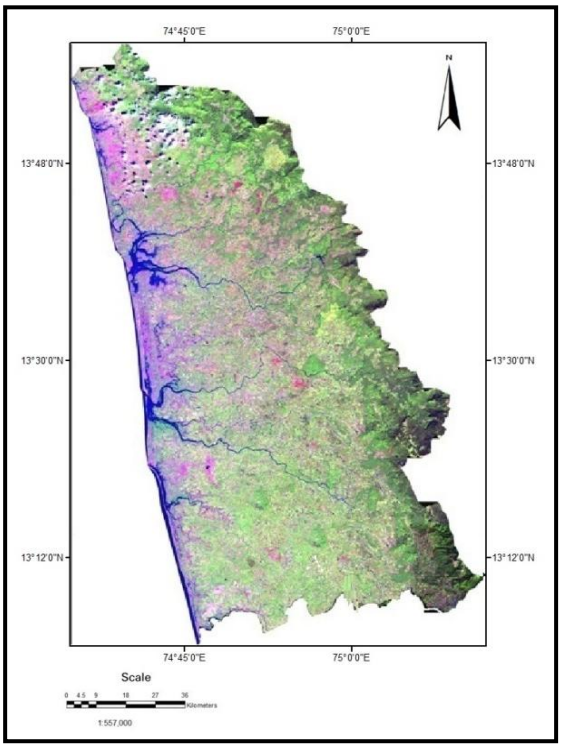

Figure 1: *Study Area as Viewed by IRS P6 – LISS IV*

3. Materials and Methods

3.1. Meteorological Data

Rainfall, temperature, pressure and relative humidity data for the year 2013 were collected from three meteorological stations of the study area namely Udupi, Karkala and Kundapura. Wind and Solar radiation data were collected from NCDC, USGS.

3.2. Satellite Data

Monthly Satellite data of MODIS sensor of Terra/Aqua Satellites were utilized for the estimation of evapotranspiration. The use of MODIS sensor data for agricultural and hydrological applications has been well recognized (Vidal and Perrier, 1989; Cristina et al., 2007). The MODIS Terra sensor data (Table 1) is acquired originally in 36 narrow wavebands. MODIS provides different sets of land products, including different levels of surface reflectance and surface temperature products. Two products namely MOD09 and MOD11A1 were acquired and re-projected using MODIS Re-projection Tool (MRT). Then, the digital numbers were converted into percent reflectance and surface temperature (LST) values using the scale factor provided with the product.

The split window technique was used to estimate surface temperature from the MODIS image. Split window algorithms calculate differential absorption in two close infrared bands to account for the effects of absorption by atmospheric gases when multiple thermal bands are available (band 31and 32).

Table 1: *MODIS Wavelength Bands and its Applications*

Band	Wavelength Range (nm)	Data Final Format	Potential Applications
1	620 – 670	Reflectance	Absolute Land cover Transformation, Vegetation Chlorophyll
2	841 – 876	Reflectance	Cloud Amount, Vegetation, Land- cover Transformation
31	10780 – 11280	Brightness Temperature	Cloud Temperature, Forest Fires & Volcanoes, Surface Temperature
32	11770 – 12270	Brightness Temperature	Cloud Height, Forest Fires & Volcanoes, Surface Temperature

3.3. Surface Energy Balance Algorithm for Land (SEBAL)

The SEBAL algorithm uses the surface energy balance to estimate aspects of the hydrological cycle. SEBAL maps evapotranspiration, biomass growth, water deficit and soil moisture.

$$LE = R_n - G - H \qquad (1)$$

Where, LE is the energy needed to change the phase of water from liquid to gas, R_n is the net radiation, G is the soil heat flux and H is the sensible heat flux. Using instruments like a scintillometer, soil heat flux plates or radiation meters, the components of the energy balance can be calculated and the energy available for actual evapotranspiration can be solved.

Surface albedo (α_s) was estimated using MODIS daily surface reflectance [2] while surface emissivity (ε_s) was estimated using MODIS NDVI composition [3].

$$\alpha_s = \sum_{b=1}^{7} [\rho_{s,b}\omega_b] \qquad (2)$$

$$\varepsilon_s = 1.009 + 0.047\, ln(\text{NDVI}) \qquad (3)$$

in which $\rho_{s,b}$ is the at-surface reflectance for band "n" and ω_b is the weighting coefficient representing the fraction of at-surface solar radiation occurring within the spectral range represented by a specific band [2].

From the residual in the instantaneous energy-balance equation and the evaporative fraction (EF) the average ET (ET_{avg}: mm·year−1) were estimated. EF has an important characteristic which is its regularity and constancy in cloud-free days [4]. Thus, its instantaneous value can be taken as the daily mean value, so that the spatial variability in average ET can be predicted over large scales.

$$EF = \frac{\mathrm{LE}}{\mathrm{R_n - G}} \qquad (4)$$

$$ET_{avg} = \frac{86400\mathrm{EFR_{n,avg}}}{\lambda} \qquad (5)$$

in which λ is the latent heat of evaporation (J·kg−1) and $R_{n,avg}$ (W·m−2) is the average net radiation balance estimated using a sinusoidal function [5], assuming that during the night Rn and the average G is zero [5,6].

$$R_{n,avg} = \frac{2\mathrm{R_n}}{\pi \sin\left[\left(\frac{\mathrm{t_{overpass} - t_{rise}}}{\mathrm{t_{set} - t_{rise}}}\right)\pi\right]} \qquad (6)$$

Where, $t_{overpass}$ (h) is the time at which the image was acquired and t_{set} (h) and t_{rise} (h) are the times of sunset and sunrise, respectively. The daytime hours were calculated based on latitude and the day of the year.

3.4. Data Integration in GIS

Satellite products and the thematic maps were integrated in GIS domain for analyzing the evapotranspiration pattern in the study area. Schematic representation of the methodology is shown in Figure 2.

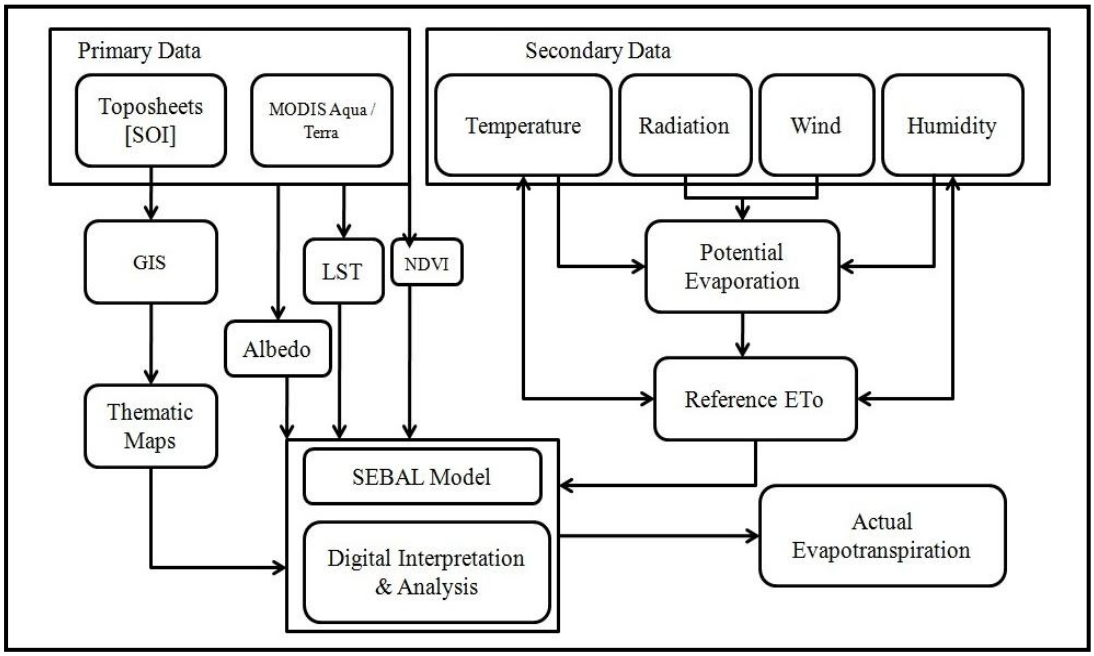

Figure 2: *Flow of Work*

4. Results and Discussion

Evapotranspiration was estimated using the SEBAL Algorithm from MODIS Satellite images and concurrent meteorological data for the year 2013 separately. The linear regression shows a good fit between 2 datasets with r^2 value of 0.9578 (Figures 14 & 15). Pearson correlation analysis yielded a correlation coefficient (t) value 0.97. Since t > 0.283 (table value) for 36 measurements at p< 0.05, the correlation is positively significant. From the study, it is clear that MODIS retrieved evapotranspiration can be directly used for the study area without modification of the retrieval algorithm. Comparison of temporal variation trend lines of two datasets confirms the above observation.

The evapotranspiration values range between 85 mm and 1230 mm for the year 2013 in the study area. The average annual evapotranspiration is shown in the Figure 11. Lower values are recorded in the month of December (Figure 13) whereas higher values are found in June (Figure 12).

Evapotranspiration is mainly dependent on vegetation cover, wind, temperature, relative humidity and elevation parameters. NDVI analysis gives indirect information on canopy cover, vegetation primary productions and phenology of vegetation classes (Amanda et al., 2013; Barbagallo et al., 2008; Yang et al., 2011). The NDVI products for the months of June and December are shown in Figures 3a & 3b respectively.

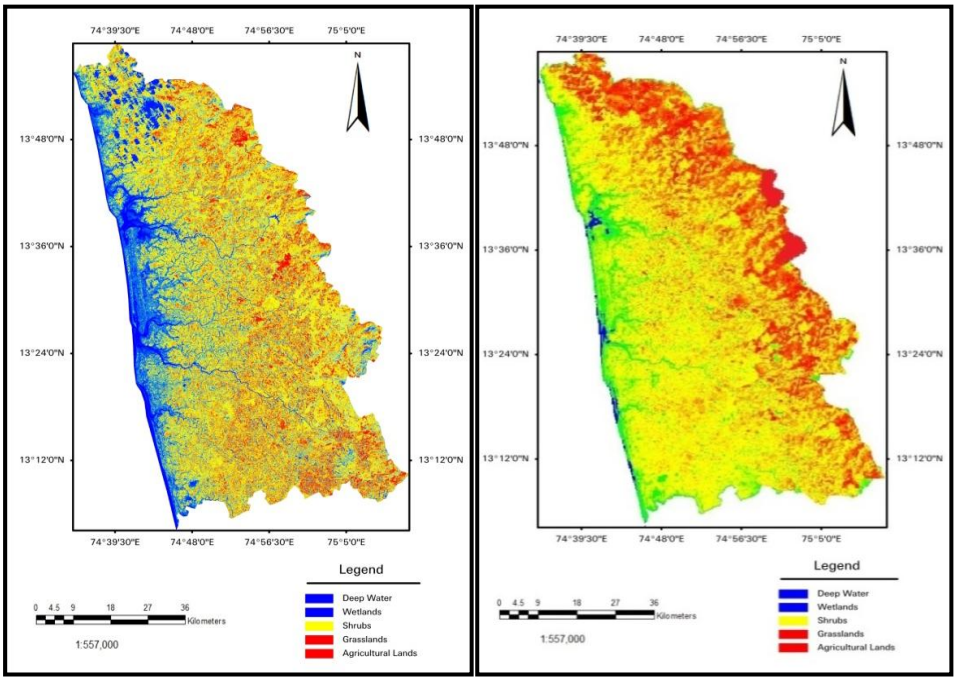

Figure 3a: *NDVI Map for the Month of June* ***Figure 3b:*** *NDVI Map for the Month of December*

Along with meteorological parameters, slope and aspect also play key role in evapotranspiration as they determine the effectiveness solar insolation. The slope map (Figure 4) and the aspect map (Figure 5) give an idea on the higher solar radiation receiving regions in the study area.

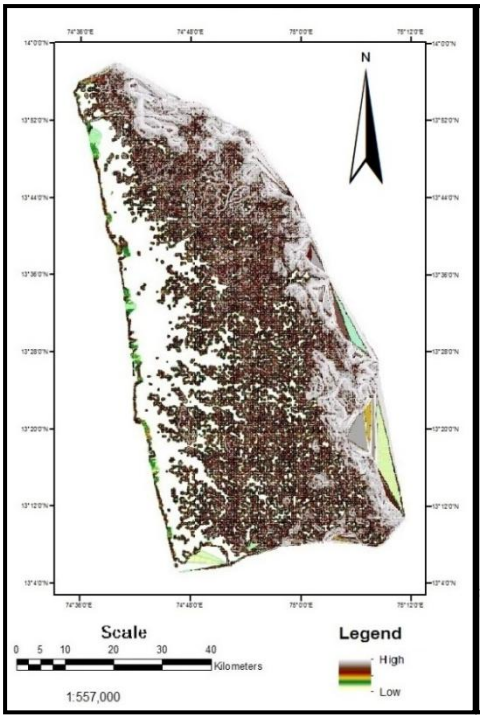

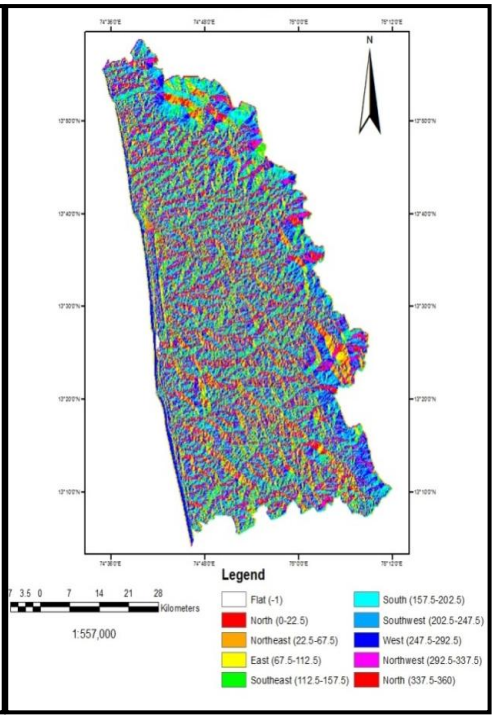

Figure 4: *Slope Map*

Figure 5: *Aspect Map*

Direct relationship between Landuse/landcover classes and evapotranspiration is observed in study (Ayoub and Ibrahim, 2008; Yong et al., 2011). Evapotranspiration is poor in coastal tract as settlements and built-up classes dominating over vegetation cover in this region. Evergreen forest, deciduous forest and grasslands are contributing for higher evapotranspiration in the study area. The landuse/landcover details are presented in Table 2.

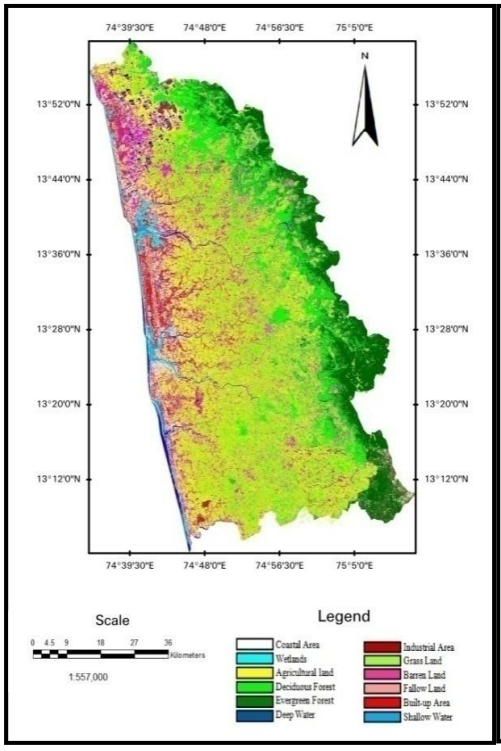

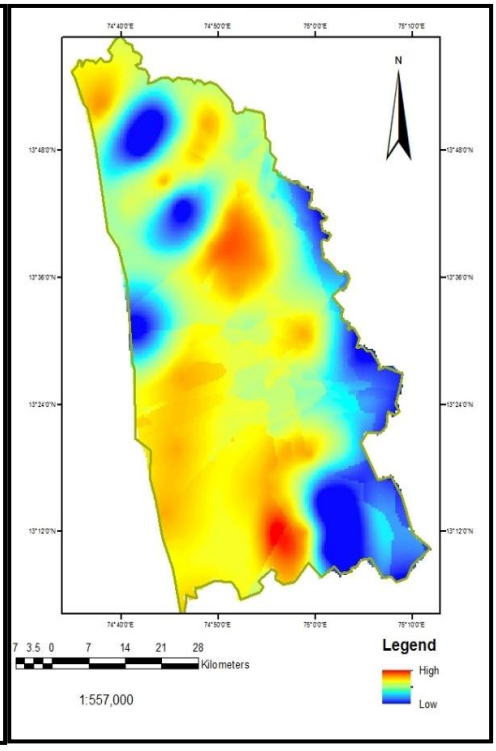

Figure 6: *Landuse / Landcover Map*

Figure 7: *Relative Humidity Map*

Integrating the landuse/landcover map (Figure 6), the evapotranspiration is classified as poor in the built-up areas moderate in the agricultural lands and plantations, good to very good in foot belt of Western Ghats. The shola forests of the study area show higher evapotranspiration.

Table 2: *Landuse/Landcover Area coverage*

S. No.	Class	Area in Sq. Km
1	Fallow Land	1383.3275
2	Shallow Water	101.91245
3	Built-up Area	758.66695
4	Coastal Area	430.9242
5	Wetlands	129.75055
6	Agricultural Land	1766.13545
7	Evergreen Forest	1456.35845
8	Deciduous Forest	2268.57485
9	Deep Water	260.63615
10	Industrial Area	222.74945
11	Barren Land	975.13955
12	Grass Land	4125.1477

The lower values of evapotranspiration reported in December (Figure 8) is attributed to lower temperature and sunshine conditions whereas the higher values reported in June (Figure 9) could be due to prevailing monsoon winds and associated high rainfall (Immerzeel and Peter, 2008; Chen et al., 2013). Northern vegetated plains of the study area show lower values through the year compared to other similar plains, which may be due to the proximity of the region to the Arabian Sea. Humidity increases towards sea (Figure 7) this in turn reduces the evapotranspiration.

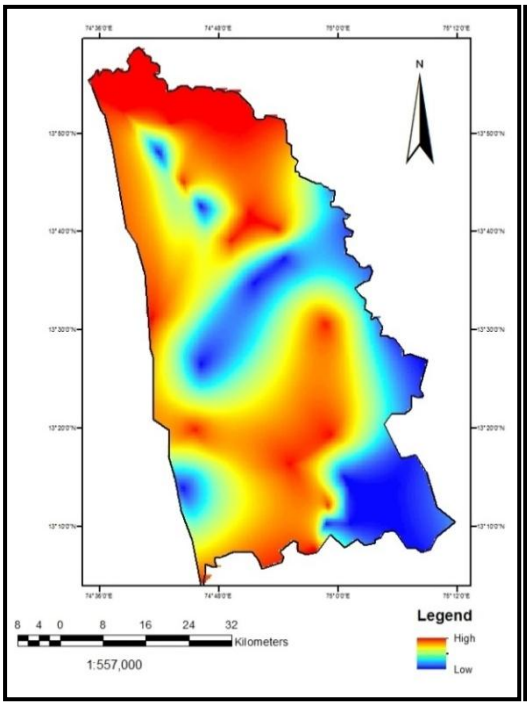

Figure 8: *Temperature Map*

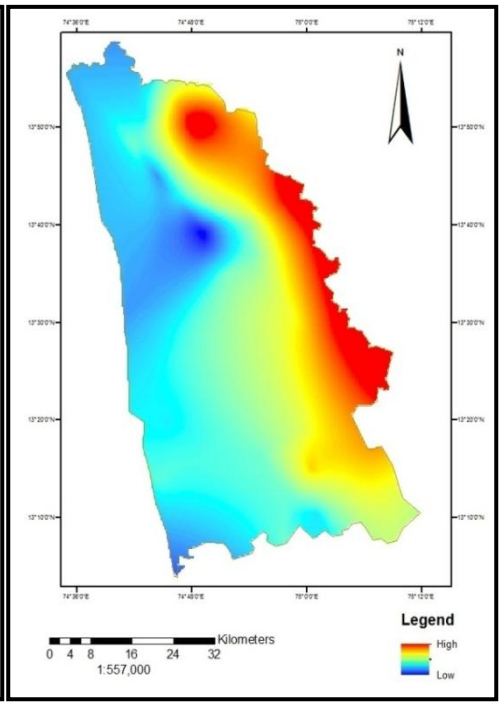

Figure 9: *Rainfall Distribution Map*

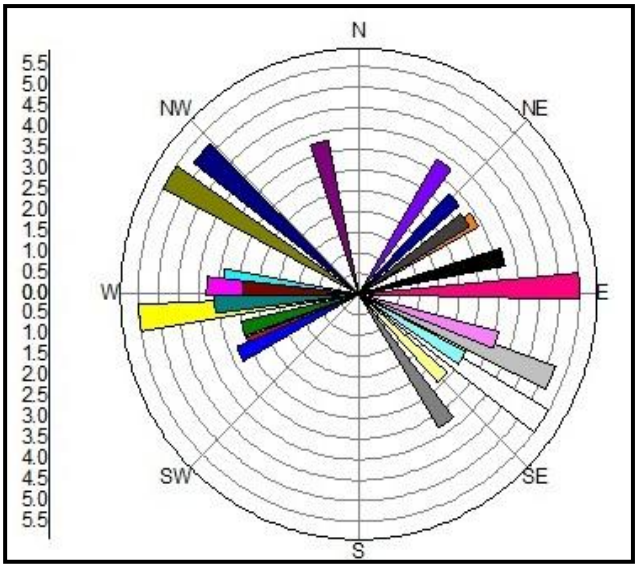

Figure 10: *Wind Rose Plot*

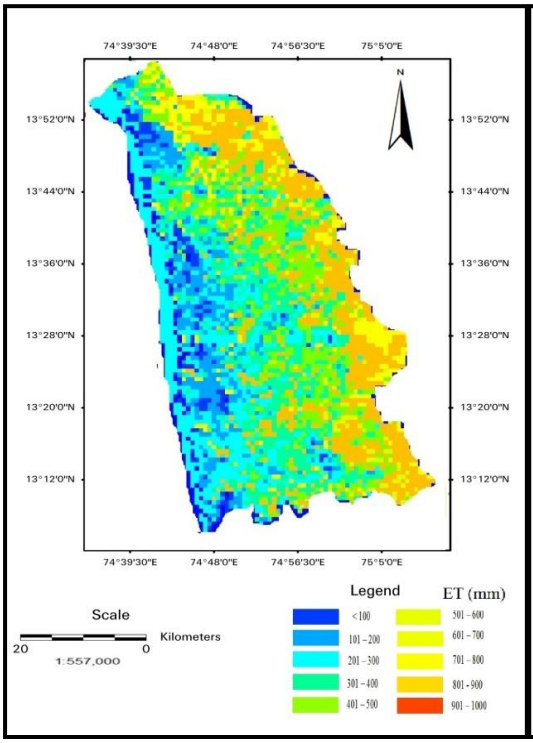

Figure 11: *Average Annual Evapotranspiration Map*

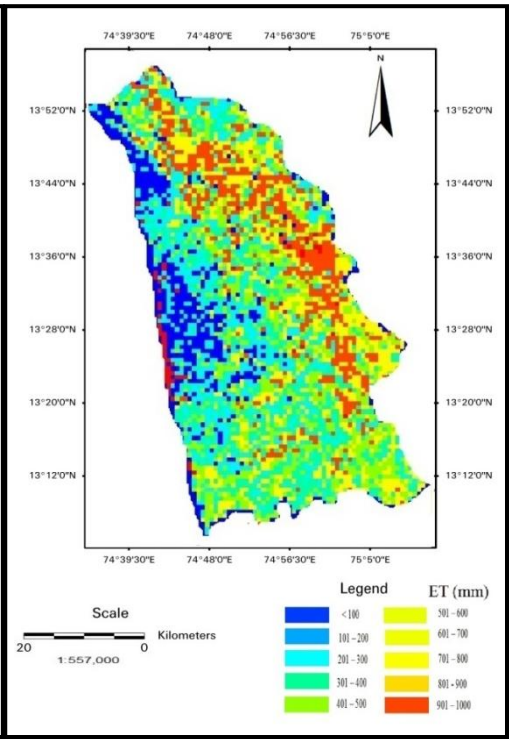

Figure 12: *Evapotranspiration Map for the Month of June*

The variations in wind direction and speed in the study area are shown in Figure 10. The wind measurements were made at a height of 10 m from ground level.

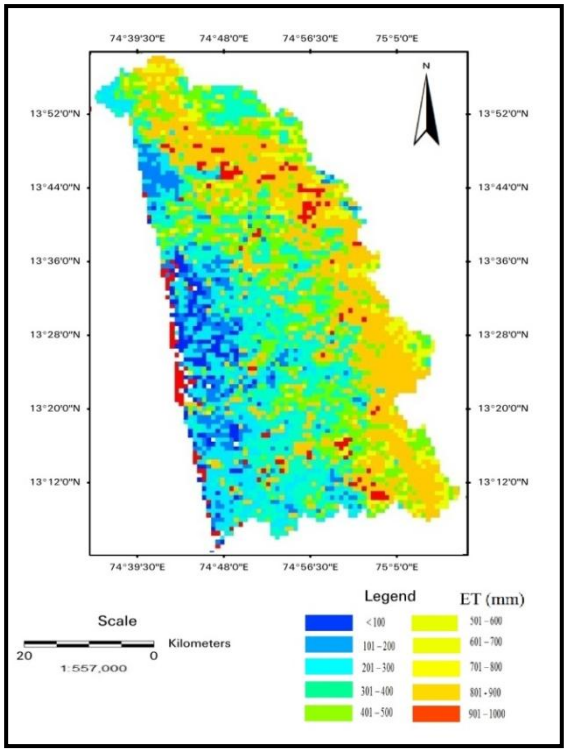

Figure 13: *Evapotranspiration Map for the Month of December*

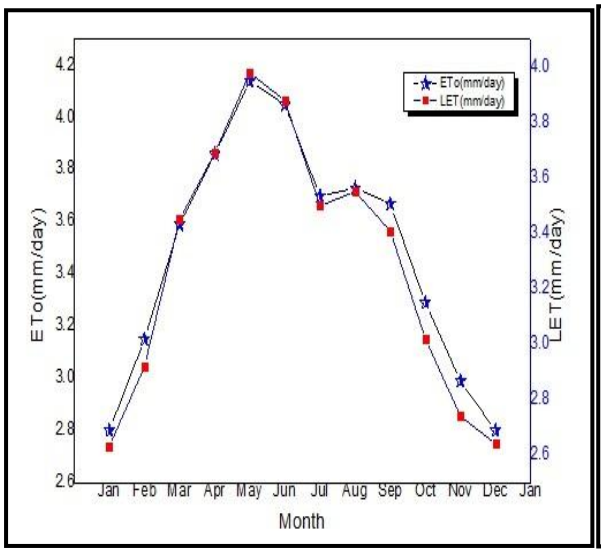

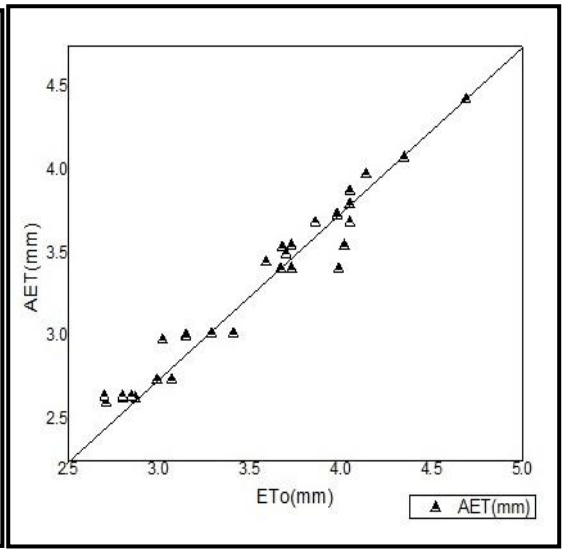

Figure 14: *Comparison of Potential ET and Actual ET* ***Figure 15:*** *Scatter plot for Actual ET and Reference ET*

A Digital Elevation Model (DEM) of the study area was prepared (Figure 16) and integrated in the study to understand the variations in evapotranspiration in relation to topography.

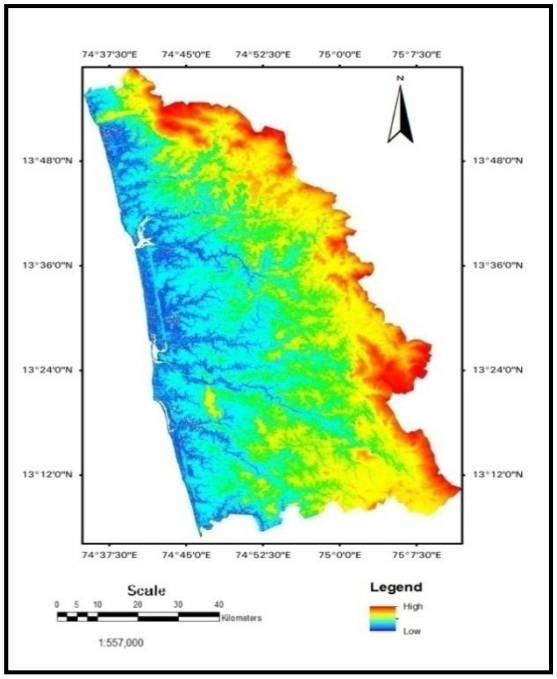

Figure 16: *DEM Map*

Lower values are found in the coastal tract especially in the areas having dense settlements followed by steep slopes of Western Ghats. The higher values are recorded along the foot belt of Western Ghats with thickly vegetated plains recording the maximum evapotranspiration.

5. Conclusion

Integration of MODIS satellite products with SEBAL algorithm is proved to be very useful in estimating evapotranspiration. Evapotranspiration is higher in the foot belt of Western Ghats and lower in the vicinity of coast. The direct relationship between landuse/landcover classes and evapotranspiration is well noticed in the study. Integration of satellite products & thematic maps in GIS domain greatly helps in understanding the spatial and temporal variations of evapotranspiration.

Acknowledgement

The authors are thankful to the Meteorological Department, Udupi district for providing the meteorological data and National Climatic Data Centre and LPDAAC, USGS for providing the MODIS sensor products.

References

Allen, R.G., Tasumi, M., and Trezza, R. *Satellite-Based Energy Balance for Mapping Evapotranspiration with Internalized Calibration (METRIC) Model*. Journal of Irrigation and Drainage Engineering. 2007. 133 (4) 380-394.

Allen, R.G., Tasumi, M., Morse, A., and Trezza, R. *A Landsat-Based Energy Balance and Evapo-Transpiration Model in Western US Water Rights Regulation and Planning.* Irrig. Drain. Syst. 2005. 19; 251-268.

Amanda Veloso, Valérie Demarez, Eric Ceschia, and Martin Claverie. *Crop Biomass and Evapotranspiration Estimation using SPOT and Formosat-2 Data.* Geophysical Research Abstracts, EGU General Assembly. 2013. 15.

Ayoub Almhab and Ibrahim Busu, 2008: *Estimation of Evapotranspiration Using Fused RS and M-SEBAL Model for Improving Water Management in Arid Mountainous Area*. 3rd International Conference on Water Resources and Arid Environments.

Barbagallo, S., Consoli, S., and Russo, A. *Estimate of Evapotranspiration using Surface Energy Fluxes from Landsat TM.* Options Méditerranéennes. 2008. 84; 105-114.

Bastiaanssen, W.G.M., 1995: *Regionalization of Surface Flux Densities and Moisture Indicators in Composite Terrain: A Remote Sensing Approach under Clear Skies in Mediterranean Climates.* Ph.D. Dissertation. Wageningen Agricultural University, Wageningen.

Bastiaanssen, W.G.M., Menenti, M., Feddes, R.A., and Holtslag, A.A.M. *A Remote Sensing Surface Energy Balance Algorithm for Land (SEBAL) Formulation.* Journal of Hydrology. 1998. 212-213; 198-212.

Brutsert, W. *Heat and Mass Transfer to and from Surface with Complete Vegetation or Similar Permeable Roughness.* Boundary Layer Meteorology. 1979. 16; 365-388.

Cristina Serban (Gherghina), Carmen Maftei, and Alina Barbulescu. *Estimation of Evapotranspiration Using Remote Sensing Data and Grid Computing: A Case Study in Dobrogea, Romania.* Latest Trends on Computers. 2007. II; 596-601.

Dawen Yang, He Chen, and Huimin Lei. *Estimation of Evapotranspiration using a Remote Sensing Model over Agricultural Land in the North China Plain*. International Journal of Remote Sensing. 2010. 31 (14) 3783-3798.

Doorenbos, J., and Pruitt, W.O. *Crop Water Requirements*. FAO Irrigation and Drainage. 1977. 24; 156.

Granger, R.J., 1997: *Comparison of Surface and Satellite-Derived Estimates of Evapotranspiration using a Feedback Algorithm*. Kite, G.W., Pietroniro, A., and Schultz T.J., (Eds). In: Applications of Remote Sensing in Hydrology. Proceedings of the 3rd International Workshop NHRI Symposium. NASA Goddard Space Flight Center, Greenbelt, MD.

Hamid Reza Matinfar. *Evapotranspiration Estimation Base upon SEBAL Model and Fieldwork*. Scholars Research Library. 2012. 3 (5) 2459-2463.

Jackson, R.J., 1967: *The Effect of Slope, Aspect and Albedo on Potential Evapotranspiration from Hill Slopes and Catchments*. Soil Bureau, D.S.I.R. 60-69.

Shiklovmanov, I.A., and Sokolov, A.A., 1983: *Methodological Basis of World Water Balance Investigation and Computation. New Approaches in Water Balance Computations*, International Association for Hydrological Sciences Publication No. 148. Proceedings of a Workshop during XVIIIth General Assembly of the International Union of Geodesy and Geophysics at Hamburg, FR Germany.

Vidal, A., and Perrier, A. *Analysis of a Simplified Relation used to Estimate Daily Evapotranspiration from Satellite Thermal IR data*. International Journal of Remote Sensing. 1989. 10 (8) 1327-1337.

Walter Immerzeel and Peter Droogers. *Calibration of a Distributed Hydrological Model Based on Satellite Evapotranspiration*. Journal of Hydrology. 2008. 394; 411-424.

Williams, D.G., Cable, W., Hultine, K., Hoedjes, J.C.B., Yepez, E.A., Simonneaux, V., Er-Raki, S., Boulet, G., de Bruin, H.A.R., and Chehbouni A. *Evapotranspiration Components Determined by Stable Isotope, Sap Flow and Eddy Covariance Techniques.* Agricultural and Forest Meteorology. 2004. 125; 241-258.

Xiao-chun Zhang, Jing-wei, W.U., Hua-yi, W.U., and Yong, L.I. *Simplified SEBAL Method for Estimating Vast Areal Evapotranspiration with MODIS Data*. Water Science and Engineering. 2011. 4 (1) 24-35.

Zhuoqi Chen, Runhe Shi, Shupeng Zhang. *An Artificial Neural Network Approach to Estimate Evapotranspiration from Remote Sensing and Ameri Flux Data.* Front. Earth Sciences. 2013. 7 (1) 103-111.